Check for updates



www.chemsuschem.org

Closo-[B₁₂H₁₂]²⁻ Derivatives with Polar Groups As Promising Building Blocks in Metal-Organic Frameworks for Gas Separation

Chuanxi Chen^{+,[a]} Zhefeng Chen^{+,[a]} Mingzheng Zhang,^[a] Shisheng Zheng,^[a] Wentao Zhang,^[a] Shunning Li,*[a] and Feng Pan*[a]

Engineering design of metal organic frameworks (MOFs) for gas separation applications is nowadays a thriving field of investigation. Based on the recent experimental studies of dodecaborate-hybrid MOFs as potential materials to separate industryrelevant gas mixtures, we herein present a systematic theoretical study on the derivatives of the closo-dodecaborate anion [B₁₂H₁₂]²⁻, which can serve as building blocks for MOFs. We discover that amino functionalization can impart a greater ability to selectively capture carbon dioxide from its mixtures

with other gases such as nitrogen, ethylene and acetylene. The main advantage lies in the polarization effect induced by amino group, which favors the localization of the negative charges on the boron-cluster anion and offers a nucleophilic anchoring site to accommodate the carbon atom in carbon dioxide. This work suggests an appealing strategy of polar functionalization to optimize the molecule discrimination ability via preferential adsorption.

Introduction

In chemical and petrochemical industry, the process of separating gas mixtures is a crucial step that often consumes a substantial amount of energy and leads to expensive production costs.[1] The traditional distillation method[2] for gas separation generally performs poorly in terms of its ability to deal with molecules with similar molecular masses.[3] Consequently, great efforts have been devoted to alternative separation techniques, among which adsorptive separation based on porous materials stands out as the most promising approach.[4] A series of porous materials such as zeolites and activated carbons have been widely explored in the past decades, but their selectivity is as yet far from satisfactory with respect to many gases.^[5] In recent years, the family of metalorganic frameworks (MOFs), which are composed of organic molecules as coordination bridges and metal ions as nodes, [6] emerges as a potential option for selective separation of industry-relevant gas mixtures. Their easily adjustable pore sizes/shapes and abundant metal sites can provide high flexibility in exploiting the optimal structures for separating different combinations of gases, [7] which endows them the unprecedented superiority over conventional materials.^[8] While the molecular sieving effects of MOFs have been extensively studied via the precise control of pore sizes and shapes, [5a,9] the mechanism of molecule discrimination via preferential adsorption is still elusive, and becomes a focus in recent studies.[10] It remains a daunting task to optimize the capability of preferential adsorption for MOFs, because complicated guest-surface interactions are likely to arise, [11] including open metal sites interaction, van der Waals interaction, and Hbonding interaction, thus leading to the difficulty in the rational design of building blocks for MOFs.

Recently, closo-dodecaborate anion [B₁₂H₁₂]²⁻ has received considerable research interest for their utility as building blocks in MOFs to separate gases such as C_2H_2/CO_2 , C_2H_6/CH_4 and C_3H_8/CO_2 CH₄. [12] Closo-[B₁₂H₁₂]²⁻ is a weakly coordinated anion with two electrons, [13] which exhibits unique properties distinguished from other organic ligands. It was reported that the H atoms on $[B_{12}H_{12}]^{2-}$ tend to form hydrogen bonds with the H atoms on gas molecules, [12a,e] and such chemical affinity could provide the decisive ability to discriminate between gases. Modification on [B₁₂H₁₂]²⁻ has also been attempted to further improve the selectivity, one example being $[B_{12}H_{11}I]^{2-}$ that exhibits much enhanced adsorption towards C₃H₈ along with weakened adsorption towards CH₄. [12c] However, systematic investigation on the interaction between $[B_{12}H_{12}]^{2-}$ derivatives and industryrelevant gases is still lacking, and there remains much to understand the role of conjugated π electrons in the boron cluster on preferential adsorption. Here, we focus on the functionality of [B₁₂H₁₂]²⁻ building blocks in MOFs and decipher how their capability of preferential adsorption is incorporated and tuned by the decoration of functional groups^[14] (Scheme 1). In these MOFs, the boron cluster coordinates with the metal ion by B-H---M bonding (M denotes the metal ion), and has B–H $^{\delta-}$...H $^{\delta+}$ –C interactions with organic ligands, thus forming a pillar node in the lattice. [12b,d] The pore sizes and shapes are tunable according to the multi-coordination between metal ions and organic ligands, which can exert considerable influence on the cooperative interactions.[15] Therefore, to

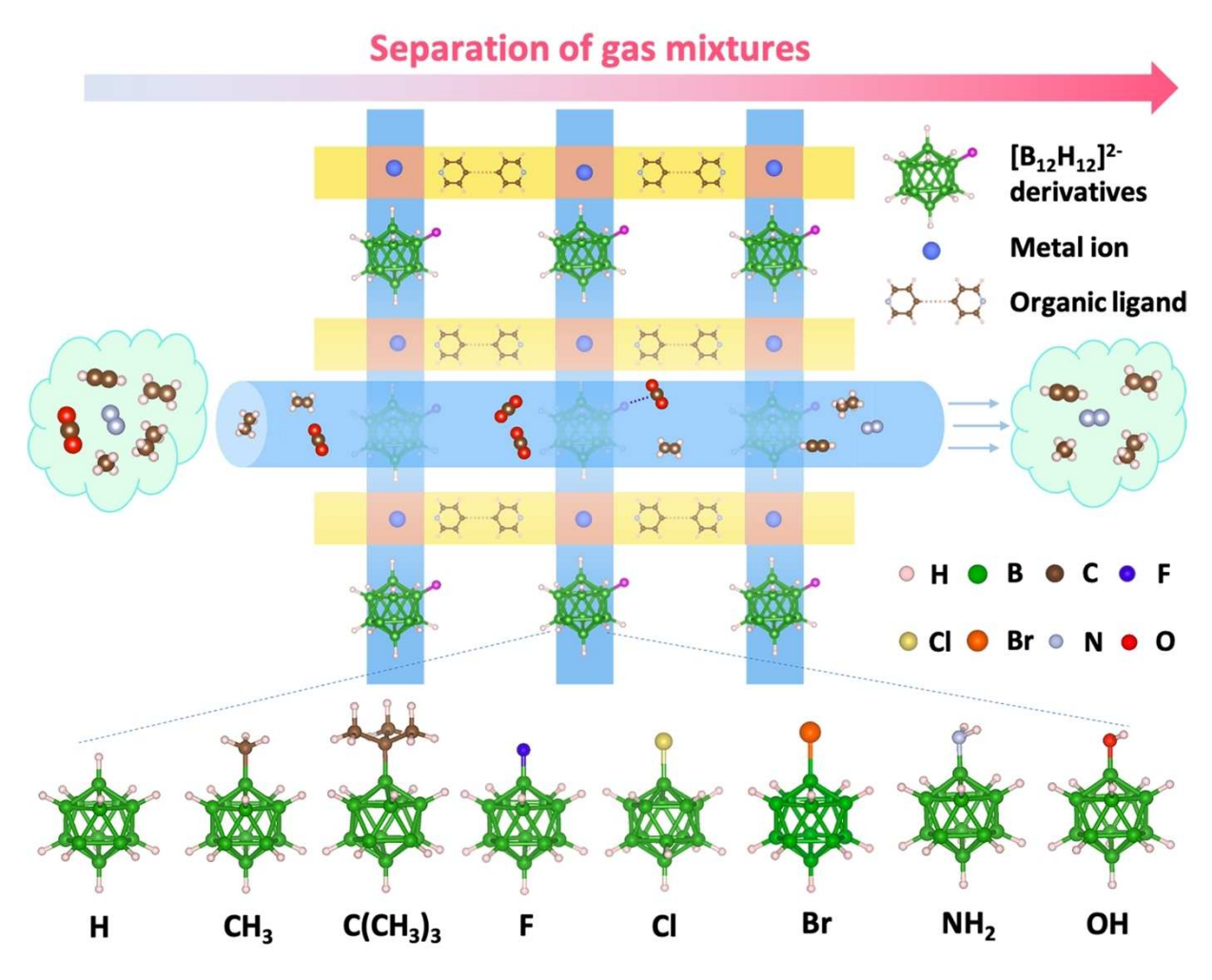
panfeng@pkusz.edu.cn

[+] These authors contributed equally to this work.

Supporting information for this article is available on the WWW under https://doi.org/10.1002/cssc.202300434

[[]a] C. Chen, * Z. Chen, * M. Zhang, S. Zheng, W. Zhang, Dr. S. Li, Prof. F. Pan School of Advanced Materials, Peking University, Shenzhen Graduate School 518055 Shenzhen (People's Republic of China) E-mail: lisn@pku.edu.cn

1, 17, Downloaded from https://chemistry-europe.online.library.wiley.com/doi/10.1002/cssc.202300434 by University Town Of Shenzhen, Wiley Online Library on [23/11/2025]. See the Terms and Conditions (https://onlinelibrary.wiley.com/enistry-europe.onlinelibrary.wiley.com/doi/10.1002/cssc.202300434 by University Town Of Shenzhen, Wiley Online Library on [23/11/2025]. See the Terms and Conditions (https://onlinelibrary.wiley.com/enistry-europe.onlinelibrary.wiley.com/doi/10.1002/cssc.202300434 by University Town Of Shenzhen, Wiley Online Library on [23/11/2025]. See the Terms and Conditions (https://onlinelibrary.wiley.com/enistry-europe.enistry-europe.enistry-europe.enistry-europe.enistry-europe.enistry-europe.enistry-europe.enistry-europe.enistry-europe.enistry-europe.enistry-europe.enist



Scheme 1. Illustration of MOFs with $closo-[B_{12}H_{12}]^{2-}$ derivatives as building blocks to facilitate gas separation.

simplify comparisons, we have simulated the isolated $[B_{12}H_{12}]^{2-}$ building blocks to examine their own contribution to preferential adsorption. A fundamental understanding of the $[B_{12}H_{12}]^{2-}$ derivatives will hopefully shed light on the selective control of gas separation in these dodecaborate-hybrid MOFs.

In this work, we perform ab initio calculations on closo- $[B_{12}H_{12}]^{2-}$ with a series of functional groups including $-CH_{3}$, -C(CH₃)₃, -F, -Cl, -Br, -NH₂ and -OH, among which the highly polarized amino group is found to be the most efficient in boosting the separation selectivity for gas mixtures, especially towards CO₂ capture. Further investigation on the electronic structures reveals that the ability of preferential adsorption mainly lies in the distribution of the two excess electrons on dodecaborate anion. These electrons are intrinsically delocalized among the boron atoms but can become relatively localized due to the polarization of the functional groups. Our results indicate that the guest-surface interactions can be predictably modified by altering the polarization in these boron-cluster building blocks, which may also be extended to the design of other porous materials for adsorptive separation of gas mixtures.

Results and Discussion

All the density functional theory calculations were carried out using Gaussian09. Two types of substitutional configurations have been examined for the decoration of functional groups (denoted as -R) on closo- $[B_{12}H_{12}]^{2-}$, as shown in Figure 1. The symmetric dual-decorated configuration is constructed for the assumption that symmetry violation on the dodecaborate anion may play a role on the adsorption energy of the gas molecules. Six kinds of gases including N₂, CO₂, C₂H₆, C₂H₄, C₂H₂ and CH₄ are taken into consideration, adding up to a total of 96 combinations of molecule and host. For each combination, five different adsorption configurations are created to fully explore the most favorable adsorption site (Figure S1). According to the free energy for the configurations after structural optimization, these molecules generally prefer to be accommodated at a location in the vicinity of the functional group while on top of the center of two or three neighboring boron atoms (Figure S2). The calculated adsorption energy in Figure 1 demonstrates that the amino group on $[B_{12}H_{12}]^{2-}$ especially favors the selective adsorption of CO₂ against other molecules. Given that an adsorption energy difference of 0.1 eV could be adequate for

1. Downloaded from https://chemistry-europe.online.library.wiley.com/doi/10.1002/cssc.202300434 by University Town Of Shenzhen, Wiley Online Library on [2311/2025]. See the Terms and Conditions (https://onlinelibrary.wiley.com/ems-and-conditions) on Wiley Online Library for rules of use; OA articles are governed by the applicable Creative Commons Licensea

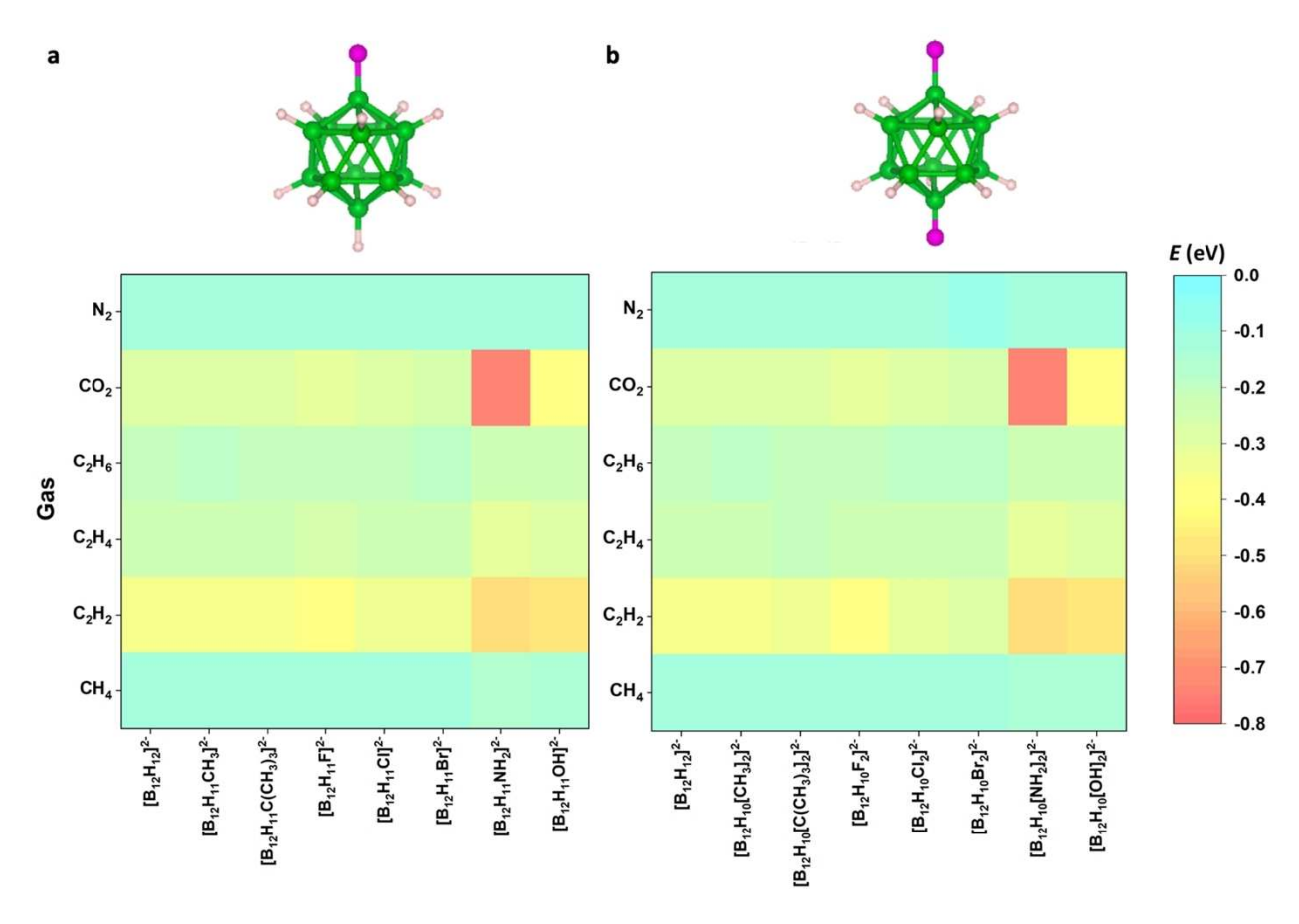


Figure 1. Adsorption energy of gas molecules on different closo-[B₁₂H₁₂]²⁻ derivatives. (a) Single-decorated configuration. (b) Symmetric dual-decorated configuration.

good performance in gas separation, [12a-e] the adsorption energy difference shown on the amino-functionalized [B₁₂H₁₂]²⁻ is large enough to guarantee much superior CO₂ selectivity than its pristine counterpart. In Tables S1-S3, we compare the gas adsorption energy and the selectivity of several reported porous materials for gas separation on CO₂/C₂H₂, CO₂/N₂ and CO₂/CH₄ systems. It is worth noting that $[B_{12}H_{11}NH_2]^{2-}$ exhibits remarkably higher adsorption energy difference than the most efficient materials in these previous studies, which highlights the potential of amino-functionalized dodecaborate component to excel in CO₂ capture. As the amino-closo-[B₁₂H₁₂]²⁻ anion has already been demonstrated experimentally synthesizable, [16] it would be ideally possible to exploit its benefits as building blocks in MOFs for gas separation applications.

An overall trend is also manifested in the adsorption energy heatmaps of Figure 1: the adsorption of gas molecules is more exothermic when the functional group on $[B_{12}H_{12}]^{2-}$ shows higher polarization. The highly polarized amino group tends to enhance the adsorption of all the gas molecules, and with the varied degree of such enhancement, a large difference is produced in the adsorption energy between CO2 and other gases. The less polarized hydroxyl group exhibits similar results but with a considerably less notable variation in adsorption energy among different gases. The polarization effect also appears in the gas molecules: those with less polar bonds (such as N₂, C₂H₆ and CH₄, based on the calculated atomic charge distribution in Table S4) show hardly any apparent change in their adsorption on different $[B_{12}H_{12}]^{2-}$ derivatives, while the polar C=O bonds in CO2 and C-H bonds in C2H2 exhibit an adsorptive behavior more sensitive to the functional groups. This implies that the preferential-adsorption ability is primarily driven by the electrostatic interaction between the gas molecule and the functional group. This hypothesis is further strengthened by the finding that the difference in adsorption energy is negligible between the single-decorated configuration (Figure 1a) and the symmetric dual-decorated one (Figure 1b). It means that not only the symmetry violation plays a trivial role, but the direct impact of conjugated $\boldsymbol{\pi}$ electrons in the boron skeleton is hardly strong enough to overwhelm the interaction between gas molecules and the functional groups, otherwise the redistribution of these π electrons upon functionalization on the far side would inevitably interfere with the energetics in gas adsorption. Thus, the adsorptive behavior of gas molecules is likely dictated by the -B-R moiety of the [B₁₂H₁₁R]²⁻ anion, which reinforces our strategy of polar functionalization on $[B_{12}H_{12}]^{2-}$ pillars in MOFs to modulate the ability of preferential adsorption.

Chemistry Europe

European Chemical Societies Publishing

3, 17, Downloaded from https://chemistry-europe.online/library.wiley.com/doi/10.1002/cssc.202300434 by University Town Of Stenzhen, Wiley Online Library on [23/11/2025]. See the Terms and Conditions (https://onlinelbrary.wiley.com/emis and-conditions) on Wiley Online Library for rules of use; OA articles are governed by the applicable Creative Commons License

Deeper insights can be gleaned from the electronic structure of the functionalized $[B_{12}H_{12}]^{2-}$ ions. We have evaluated the partial atomic charges of the single-decorated $[B_{12}H_{11}R]^{2-}$ (Figure 2a) via the CHELPG scheme, which has previously proved reliable in the analysis of borane clusters.[18] Here, for each kind of functional group, the atom binding to the boron skeleton is taken as the representative. The extraction of electron from the boron skeleton to this representative atom could be regarded as a signature of polarization in the -B-R moiety. Notably, the amino N atom and the hydroxyl O atom, as distinct from the representative atom of any other functional group, can strongly withdraw electron density from their neighboring atoms, from which we can expect an increased degree of electron localization. This scenario is well illustrated in the comparison of electrostatic potentials shown in Figures 2b and c. In $[B_{12}H_{12}]^{2-}$, the two excess electrons are nearly evenly distributed in the entire cluster, with H atoms having a slightly larger proportion. This homogeneous charge distribution is violated by the amino functionalization, whose nonbonding electron pair exhibits a highly nucleophilic character, thus providing a selective anchoring site for those gas molecules with polar bonds. However, it does not follow that the amino functional group alone can dictate the electrostatic interaction with gas molecules. As we will see in the results below, the adsorptive behavior of molecules is intimately linked to the subtle interplay between the decorated functional groups and the conjugated π electrons in the boron cluster.

To better understand this interplay, we have examined the molecular orbitals of the $[B_{12}H_{12}]^{2-}$ derivatives. The energy-level alignment of frontier molecular orbitals are studied at the B3LYP/6-311G(d,p) level of theory, which has been wellrecognized to be adequate for predicting accurate electronic structure. As displayed in Figure 3, the highest occupied molecular orbital (HOMO) of $[B_{12}H_{12}]^{2-}$ is comprised of four-fold degenerate states, which are filled by both the inherent electrons of the cluster and the two excess electrons due to the dual negative charges. The four-fold degeneracy is split into two two-fold degeneracies when it is functionalized by -CH₃, -C(CH₃)₃, -F, -Cl, or -Br. The lower-lying degenerate states are spread along the horizontal direction of the boron cluster, while the higher-lying states are along the vertical direction with broken symmetry. When decorated with either -NH2 or -OH group, the cluster becomes rotationally asymmetric, and consequently the higher-lying doublet states are split. An interesting feature of this splitting is the shifting of HOMO to a much higher energy level, especially for the case of -NH2. In

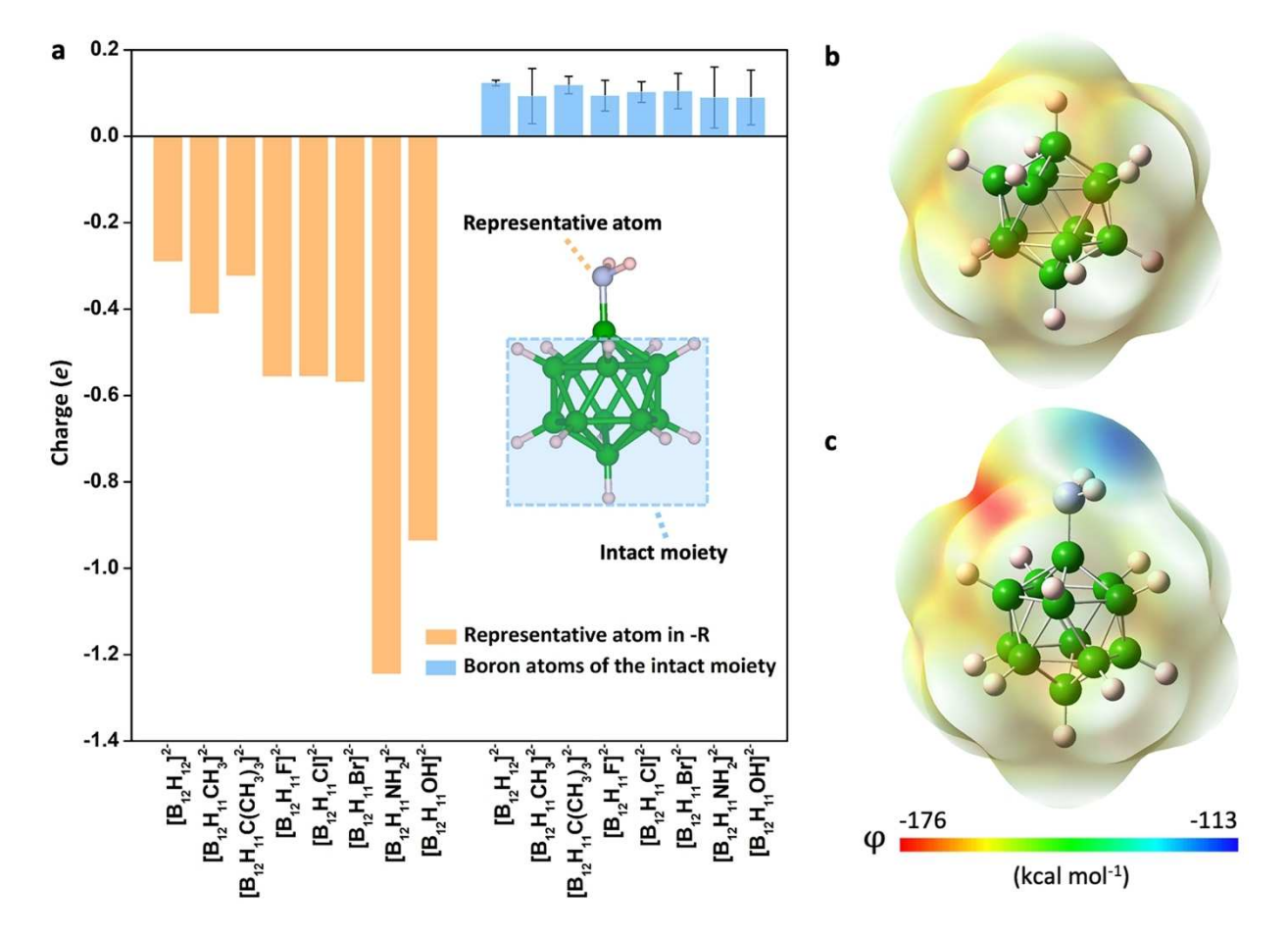


Figure 2. Charge distribution in closo-[B₁,H₁,]²⁻ derivatives. (a) Partial atomic charge of the representative atom in the functional group (denoted as –R), and the average partial atomic charge of boron atoms of the intact moiety (i.e., all boron atoms except for the one binding to the functional group). Electrostatic potential distributions of (b) $[B_{12}H_{12}]^{2-}$ and (c) $[B_{12}H_{11}NH_2]^{2-}$.

s, 17, Downloaded from https://chemistry-europe.online/lbrary.wiley.com/doi/10.1002/cssc.202300434 by University Town Of Stenzhen, Wiley Online Library on [23/11/2023]. See the Terms and Conditions (https://onlinelbrary.wiley.com/ems

and-conditions) on Wiley Online Library for rules of use; OA articles are governed by the applicable Creative Commons License

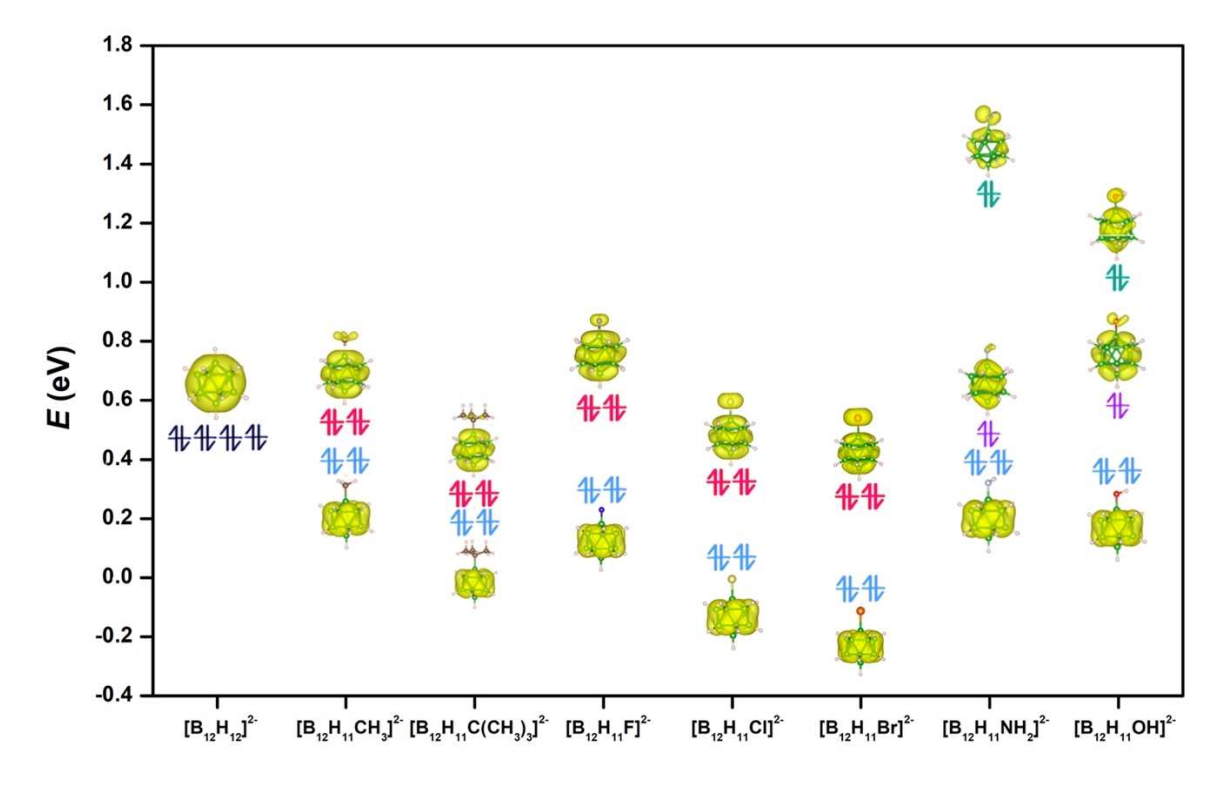


Figure 3. HOMO levels of *closo*-[B₁₂H₁₂]²⁻ derivatives and the corresponding orbital diagrams.

contrast to the drastic change of HOMO after functionalization, the change of the lowest unoccupied molecular orbital (LUMO) is almost negligible (Figure S3), leading to a significantly decreased energy gap between HOMO and LUMO upon –NH₂/ –OH functionalization. Given the notable reduction of the adsorption energy for both kinds of functional groups, our results are overall in line with the previous studies demonstrating that preferential adsorption is closely related with the band gap of the host material.^[19]

It is important to note that for all the $[B_{12}H_{12}]^{2-}$ derivatives considered in this work, their HOMO levels are all contributed by both the boron cluster and the functional groups, with the former being the major part (Figure S4). Due to the negative charges on these $[B_{12}H_{11}R]^{2-}$ anions, they have a much-boosted affinity to atoms having net positive charges, especially those in molecules bearing strongly polar bonds. The partial localization of the negative charges onto the functional groups will apparently promote this affinity, which is even more prominent when the electrons in the filled orbitals of $[B_{12}H_{11}R]^{2-}$ can transfer to the empty orbitals of the gas molecules. The up-lift of HOMO in amino functionalization will facilitate such transfer and is thus responsible for the highly exothermic energy for CO_2 adsorption.

This electron transfer can be further described by the differential charge density diagrams as shown in Figure 4. The differential charge density is constructed by subtracting the total electron densities of both the $[B_{12}H_{11}R]^{2-}$ cluster and the isolated gas molecule from that of the adsorption configuration without modifying the atomic positions. Charge redistribution is clearly seen in the C_2H_2 and CO_2 molecules, indicating the

polarization effect imposed by the excess electrons on the dodecaborate ion. While the degree of redistribution is almost the same between $[B_{12}H_{12}]^{2-}$ and $[B_{12}H_{11}F]^{2-}$, it becomes more intense in the case of $[B_{12}H_{11}NH_2]^{2-}$, which is commensurate with the amount of charge transfer as predicted by CHELPG scheme (Tables S5 and S6). We note that the charge transfer between amino functional group and CO_2 molecule reaches 0.56 e, whereas the corresponding value is below 0.1 e for $[B_{12}H_{11}F]^{2-}$. The differential charge density diagrams also justify our conclusion that the partial localization of the negative charges on the dodecaborate ion could boost the electrostatic attractive forces on molecules through the effective accommodation of their positively charged atoms.

The role of the excess electrons in $[B_{12}H_{12}]^{2-}$ can be understood in a more straightforward way by the comparison with carborane $C_2B_{10}H_{12}$ which is electrically neutral. The adsorption energy of CO₂ on C₂B₁₀H₁₂ is provided in Figure 5, with the structure of adsorption configuration depicted in Figure S5. We also examine the effect of amino functionalization. It is interesting to find that the adsorption energy follows the order of $C_2B_{10}H_{12} > C_2B_{10}H_{11}NH_2 > [B_{12}H_{12}]^{2-} > [B_{12}H_{11}NH_2]^{2-}$, and the amino functionalization on $C_2B_{10}H_{12}$ only results in an adsorption energy 0.07 eV more negative than the pristine structure. The comparatively huge difference in adsorption energy between $C_2B_{10}H_{11}NH_2$ and $[B_{12}H_{11}NH_2]^{2-}$ (above 0.5 eV) indicates that the non-bonding electron pair on amino group itself plays a much less critical role than the excess electrons on the boron cluster, which lends strong support to our electronic structure analysis that the adsorptive behavior of gases relies on the partial localization of negative charges in the host

1, 17, Downloaded from https://chemistry-europe.online.library.wiley.com/doi/10.1002/cssc.202300434 by University Town Of Shenzhen, Wiley Online Library on [23/11/2025]. See the Terms and Conditions (https://onlinelibrary.wiley.com/enistry-europe.onlinelibrary.wiley.com/doi/10.1002/cssc.202300434 by University Town Of Shenzhen, Wiley Online Library on [23/11/2025]. See the Terms and Conditions (https://onlinelibrary.wiley.com/enistry-europe.onlinelibrary.wiley.com/doi/10.1002/cssc.202300434 by University Town Of Shenzhen, Wiley Online Library on [23/11/2025]. See the Terms and Conditions (https://onlinelibrary.wiley.com/enistry-europe.enistry-europe.enistry-europe.enistry-europe.enistry-europe.enistry-europe.enistry-europe.enistry-europe.enistry-europe.enistry-europe.enistry-europe.enist

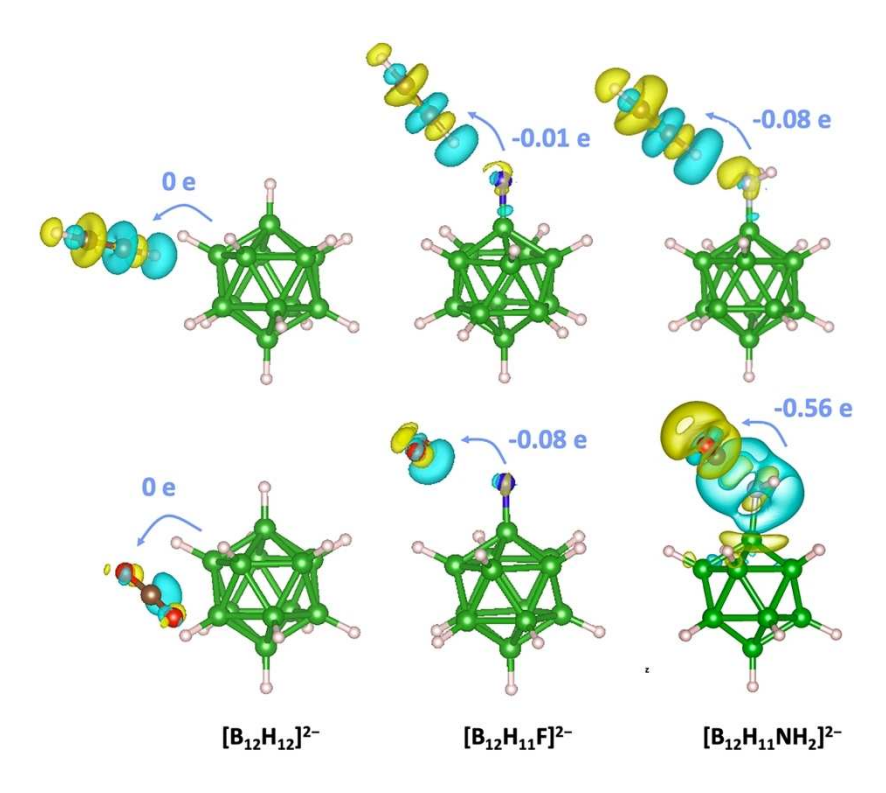


Figure 4. Differential charge density distributions in the adsorption of C_2H_2 (upper panel) and CO_2 (lower panel) on $[B_{12}H_{12}]^{2-}$, $[B_{12}H_{11}F]^{2-}$ and $[B_{12}H_{11}NH_2]^{2-}$. The isosurface was set at 0.002 $e^{\frac{A}{A}-3}$, and the yellow/blue areas represent a gain/loss of electrons.

material. This insight is also corroborated by the relatively high adsorption energy of CO₂ on C₆H₅NH₂, C₂H₅NH₂ and CH₃NH₂, as shown in Figure S6. Extending from this, we can foresee that host materials with a higher propensity to maintain a delocalized electronic state are likely to be less effective in capturing CO2. This is substantiated by our calculations for the negatively charged fullerene ions shown in Figure 5. The excess electrons tend to be homogeneously distributed among the carbon atoms, similar to $[B_{12}H_{12}]^{2-}$. However, in contrast to the latter, the large size of fullerene will to some extent hinder the electron localization onto the amino functional group, and correspondingly, much less affinity to CO₂ is observed. Likewise, in case of small size clusters such as $[B_{10}H_{10}]^{2-}$ (Figure S7), amino functionalization could even lead to a more exothermic energy (-0.81 eV) than that of $[B_{12}H_{11}NH_2]^{2-}$ (-0.75 eV) for CO_2 adsorption. According to the above results, the synergy between the electrons in boron cluster and the decorated functional group can therefore be recognized as the root cause of the variation in preferential-adsorption ability of the $[B_{12}H_{12}]^{2-}$ derivatives.

Conclusions

A series of $[B_{12}H_{12}]^{2-}$ derivatives are systematically investigated via ab initio calculations to identify those with the potential of separating industry-relevant gas mixtures via preferential adsorption. Among all the functional groups considered in this work, the amino group is distinguished from the others by its

strong polarization that enables the partial localization of the negative charges on the dodecaborate anion. By virtue of the synergy between the conjugated π electrons in the boron cluster and the nucleophilic character of the amino group, $[B_{12}H_{11}NH_2]^{2-}$ exhibits a high selectivity in capturing CO_2 from its mixtures with other gases including N_2 , C_2H_6 , C_2H_4 , C_2H_2 and CH_4 . This work unfolds the promising future of dodecaborate-hybrid MOFs that use highly polar $[B_{12}H_{12}]^{2-}$ derivatives as the building blocks to facilitate gas separation.

Computational Method

The structures of $[B_{12}H_{11}R]^{2-}$ and $[B_{12}H_{10}R_2]^{2-}$ $(R=-H,-CH_3,-C(CH_3)_3,-F,-CI,-Br,-NH_2, and-OH)$ were optimized by Gaussian09^[20] using B3LYP-D3 and 6-311+G(d, p) basis set. [21] Frequency calculations were performed to examine the stability after geometry optimization. The molecular orbitals were exported from the wave function files using GaussView 5. [22] Structures were displayed using the VESTA software. [23] The absorption energy of gas molecules on closo-[B₁₂H₁₂]²⁻ was calculated using Equation (1), where $E_{cluster+gas}$ $E_{cluster}$ and E_{gas} are the total energies of the adsorption configuration, the boron cluster and the gas molecular, respectively.

$$E_{\rm ad} = E_{\rm cluster+gas} - E_{\rm cluster} - E_{\rm gas} \tag{1}$$

For each combination of gas and host, five different adsorption configurations were evaluated, and only the configuration with the lowest total energy was adopted for investigation. Charge distributions were computed via the natural population analysis and



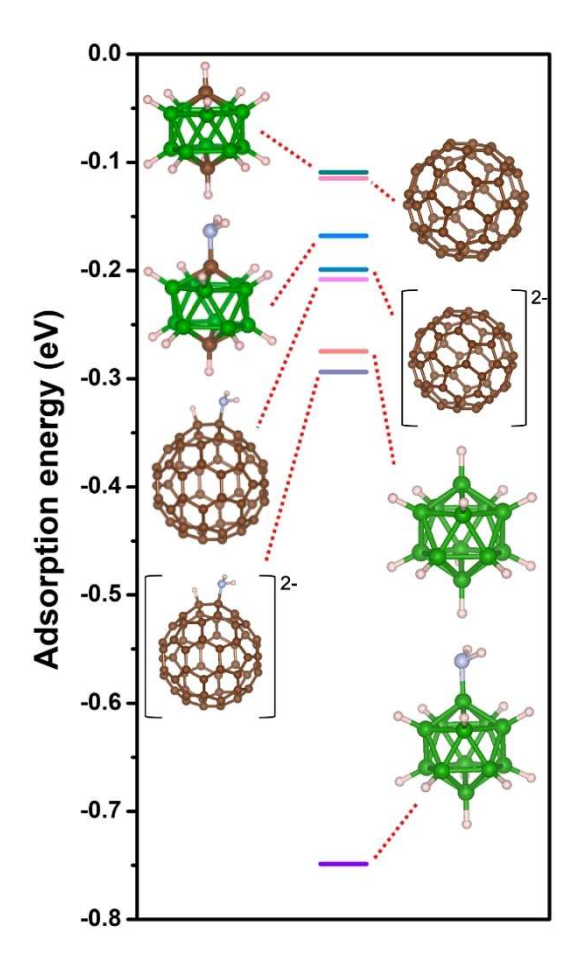


Figure 5. Adsorption energy of CO_2 on $[B_{12}H_{12}]^{2-}$, $[B_{12}H_{11}NH_2]^{2-}$, $C_2B_{10}H_{12}$, $C_2B_{10}H_{11}NH_2$, C_6 , C_6HNH_2 , $[C_6]^{2-}$ and $[C_{60}HNH_2]^{2-}$.

CHELPG (charges from electrostatic potentials using a grid) method. [17] Charge density difference and orbital composition were computed using multiwfn software. [24]

Supporting Information

Supplementary data to this article can be found online.

Acknowledgements

This work was financially supported by the Guangdong Basic and Applied Basic Research Foundation (2020 A1515110843), Young S&T Talent Training Program of Guangdong Provincial Association for S&T (SKXRC202211), Soft Science Research Project of Guangdong Province (No. 2017B030301013), National Natural Science Foundation of China (22109003) and the Major Science and Technology Infrastructure Project of Material Genome Big-science Facilities Platform supported by Municipal Development and Reform Commission of Shenzhen.

Conflict of Interests

The authors declare no conflict of interest.

Data Availability Statement

The data that support the findings of this study are available from the corresponding author upon reasonable request.

Keywords: Ab initio calculations \cdot Boron cluster \cdot Carbon dioxide capture \cdot Gas separation \cdot Metal organic frameworks

- [1] D. S. Sholl, R. P. Lively, Nature 2016, 532, 435-437.
- [2] a) C. J. King, in Separation processes, Courier Corporation, Chelmsford, 2013; b) B. L. Karger, L. R. Snyder, C. Horvath, in Introduction to separation science, New York, 1973.
- [3] Z. Bao, G. Chang, H. Xing, R. Krishna, Q. Ren, B. Chen, *Energy Environ. Sci.* 2016, 9, 3612–3641.
- [4] a) S. Chu, Y. Cui, N. Liu, Nat. Mater. 2017, 16, 16–22; b) L. Yang, S. Qian,
 X. Wang, X. Cui, B. Chen, H. Xing, Chem. Soc. Rev. 2020, 49, 5359–5406.
- [5] a) R. T. Yang, in Adsorbents: fundamentals and applications, John Wiley & Sons, New Jersey, 2003; b) R. T. Yang, in Gas separation by adsorption processes, Singapore, World Scientific, 1997.
- [6] H.-C. Zhou, J. R. Long, O. M. Yaghi, Chem. Rev. 2012, 112, 673–674.
- [7] a) C. Sanchez, B. Julián, P. Belleville, M. Popall, J. Mater. Chem. 2005, 15, 3559-3592; b) H. Wang, X. Dong, V. Colombo, Q. Wang, Y. Liu, W. Liu, X. L. Wang, X. Y. Huang, D. M. Proserpio, A. Sironi, Adv. Mater. 2018, 30, 1805088; c) H. Wang, Y. Liu, J. Li, Adv. Mater. 2020, 32, 2002603; d) X. Wang, Z. Niu, A. M. Al-Enizi, A. Nafady, Y. Wu, B. Aguila, G. Verma, L. Wojtas, Y.-S. Chen, Z. Li, J. Mater. Chem. A. 2019, 7, 13585-13590; e) W. Xu, B. Tu, Q. Liu, Y. Shu, C.-C. Liang, C.S. Diercks, O.M. Yaghi, Y.-B. Zhang, H. Deng, Q. Li, Nat. Rev. Mater. 2020, 5, 764-779; f) Z. Chen, P. Li, R. Anderson, X. Wang, X. Zhang, L. Robison, L. R. Redfern, S. Moribe, T. Islamoglu, D. A. Gómez-Gualdrón, Science 2020, 368, 297-303; g) H. K. Chae, D. Y. Siberio-Pérez, J. Kim, Y. Go, M. Eddaoudi, A. J. Matzger, M. O'Keeffe, O. M. Yaghi, Nature 2004, 427, 523-527; h) H. Li, M. Eddaoudi, M. O'Keeffe, O. M. Yaghi, Nature 1999, 402, 276-279; i) M. Eddaoudi, J. Kim, N. Rosi, D. Vodak, J. Wachter, M. O'Keeffe, O. M. Yaghi, Science 2002, 295, 469-472; j) A. Knebel, J. Caro, Nat. Nanotechnol. 2022, 17, 911-923; k) C. Wang, Y. Sun, L. Li, R. Krishna, T. Ji, S. Chen, J. Yan, Y. Liu, Angew. Chem. 2022, 134, e202203663; I) Y. Sun, J. Yan, Y. Gao, T. Ji, S. Chen, C. Wang, P. Lu, Y. Li, Y. Liu, Angew. Chem. Int. Ed. 2023, 62, e202216697.
- [8] a) R.-B. Lin, S. Xiang, W. Zhou, B. Chen, Chem 2020, 6, 337–363; b) D. N. Dybtsev, H. Chun, S. H. Yoon, D. Kim, K. Kim, J. Am. Chem. Soc. 2004, 126, 32–33; c) D. G. Samsonenko, H. Kim, Y. Sun, G. H. Kim, H. S. Lee, K. Kim, Chem. Asian J. 2007, 2, 484–488; d) M. Dinca, J. R. Long, J. Am. Chem. Soc. 2005, 127, 9376–9377; e) R. Matsuda, R. Kitaura, S. Kitagawa, Y. Kubota, R. V. Belosludov, T. C. Kobayashi, H. Sakamoto, T. Chiba, M. Takata, Y. Kawazoe, Nature 2005, 436, 238–241; f) X. Lin, A. J. Blake, C. Wilson, X. Z. Sun, N. R. Champness, M. W. George, P. Hubberstey, R. Mokaya, M. Schröder, J. Am. Chem. Soc. 2006, 128, 10745–10753; g) X. Cui, K. Chen, H. Xing, Q. Yang, R. Krishna, Z. Bao, H. Wu, W. Zhou, X. Dong, Y. Han, Science 2016, 353, 141–144; h) H. C. Gulbalkan, Z. P. Haslak, C. Altintas, A. Uzun, S. Keskin, Chem. Eng. J. 2022, 428, 131239; i) A. N. Hong, H. Yang, X. Bu, P. Feng, EnergyChem 2022, 4, 100080.
- [9] a) J. U. Keller, R. Staudt, in Gas adsorption equilibria: experimental methods and adsorptive isotherms, Springer Science & Business Media, Berlin, 2005; b) P. Nugent, Y. Belmabkhout, S. D. Burd, A. J. Cairns, R. Luebke, K. Forrest, T. Pham, S. Ma, B. Space, L. Wojtas, Nature 2013, 495, 80–84; c) Y. Jiang, J. Hu, L. Wang, W. Sun, N. Xu, R. Krishna, S. Duttwyler, X. Cui, H. Xing, Y. Zhang, Angew. Chem. Int. Ed. 2022, 61, e202200947; d) J. Wang, Y. Zhang, Y. Su, X. Liu, P. Zhang, R.-B. Lin, S. Chen, Q. Deng, Z. Zeng, S. Deng, Nat. Commun. 2022, 13, 200; e) S. Zhou, O. Shekhah, A. Ramírez, P. Lyu, E. Abou-Hamad, J. Jia, J. Li, P. M. Bhatt, Z. Huang, H. Jiang, Nature 2022, 606, 706–712; f) J. Yang, M. Tong, G. Han, M. Chang, T. Yan, Y. Ying, Q. Yang, D. Liu, Adv. Funct. Mater. 2023, 33, 2213743.



- [10] a) N. Nijem, P. Thissen, Y. Yao, R. C. Longo, K. Roodenko, H. Wu, Y. Zhao, K. Cho, J. Li, D. C. Langreth, J. Am. Chem. Soc. 2011, 133, 12849-12857; b) J. W. Yoon, Y. K. Seo, Y. K. Hwang, J. S. Chang, H. Leclerc, S. Wuttke, P. Bazin, A. Vimont, M. Daturi, E. Bloch, Angew. Chem. Int. Ed. 2010, 49, 5949-5952; c) R.-B. Lin, H. Wu, L. Li, X.-L. Tang, Z. Li, J. Gao, H. Cui, W. Zhou, B. Chen, J. Am. Chem. Soc. 2018, 140, 12940-12946; d) Y. Ye, S. Xian, H. Cui, K. Tan, L. Gong, B. Liang, T. Pham, H. Pandey, R. Krishna, P. C. Lan, J. Am. Chem. Soc. 2021, 144, 1681-1689; e) X. Cao, Z. Wang, Z. Qiao, S. Zhao, J. Wang, ACS Appl. Mater. Interfaces 2019, 11, 5306-5315; f) C. M. Cunningham, D. S. Chapin, H. L. Johnston, J. Am. Chem. Soc. 1958, 80, 2382-2384; g) A. Javaid, Chem. Eng. J. 2005, 112, 219-226; h) X. Wang, Y. Wu, J. Peng, Y. Wu, J. Xiao, Q. Xia, Z. Li, Chem. Eng. J. 2019, 358, 1114-1125; i) X. Xu, X. Zhao, L. Sun, X. Liu, J. Nat. Gas Chem. 2009, 18, 167–172; j) X.-W. Gu, J.-X. Wang, E. Wu, H. Wu, W. Zhou, G. Qian, B. Chen, B. Li, J. Am. Chem. Soc. 2022, 144, 2614–2623; k) R. Sahoo, S. Mondal, D. Mukherjee, M. C. Das, Adv. Funct. Mater. 2022, 32, 2207197; l) Y. Jiang, Y. Hu, B. Luan, L. Wang, R. Krishna, H. Ni, X. Hu, Y. Zhang, Nat. Commun. 2023, 14, 401.
- [11] a) K. Sumida, D. L. Rogow, J. A. Mason, T. M. McDonald, E. D. Bloch, Z. R. Herm, T.-H. Bae, J. R. Long, Chem. Rev. 2012, 112, 724-781; b) C. A. Trickett, A. Helal, B. A. Al-Maythalony, Z. H. Yamani, K. E. Cordova, O. M. Yaghi, Nat. Rev. Mater. 2017, 2, 1-16; c) J. Yu, L.-H. Xie, J.-R. Li, Y. Ma, J. M. Seminario, P. B. Balbuena, Chem. Rev. 2017, 117, 9674-9754; d) T. M. McDonald, D. M. D'Alessandro, R. Krishna, J. R. Long, Chem. Sci. 2011, 2, 2022-2028; e) L. J. Murray, M. Dinca, J. Yano, S. Chavan, S. Bordiga, C. M. Brown, J. R. Long, J. Am. Chem. Soc. 2010, 132, 7856-7857; f) D. Britt, D. Tranchemontagne, O. M. Yaghi, Proc. Nat. Acad. Sci. 2008, 105, 11623-11627; g) A. Demessence, D. M. D'Alessandro, M. L. Foo, J. R. Long, J. Am. Chem. Soc. 2009, 131, 8784-8786; h) W. You, Y. Liu, J. D. Howe, D. Tang, D. S. Sholl, J. Phys. Chem. C. 2018, 122, 27486-27494; i) K.-J. Chen, H. S. Scott, D. G. Madden, T. Pham, A. Kumar, A. Bajpai, M. Lusi, K. A. Forrest, B. Space, J. J. Perry, Chem 2016, 1, 753-765; j) F. Luo, C. Yan, L. Dang, R. Krishna, W. Zhou, H. Wu, X. Dong, Y. Han, T.-L. Hu, M. O'Keeffe, J. Am. Chem. Soc. 2016, 138, 5678-5684; k) W. Gong, H. Cui, Y. Xie, Y. Li, X. Tang, Y. Liu, Y. Cui, B. Chen, J. Am. Chem. Soc. 2021, 143, 14869-14876; I) L. Yang, L. Yan, W. Niu, Y. Feng, Q. Fu, S. Zhang, Y. Zhang, L. Li, X. Gu, P. Dai, *Angew. Chem.* **2022**, *134*, e202204046; m) C. Zhang, X. Dong, Y. Chen, H. Wu, L. Yu, K. Zhou, Y. Wu, Q. Xia, H. Wang, Y. Han, Sep. Purif. Technol. 2022, 291, 120932; n) G.-D. Wang, J. Chen, Y.-Z. Li, L. Hou, Y.-Y. Wang, Z. Zhu, Chem. Eng. J. 2022, 433, 133786; o) G. D. Wang, R. Krishna, Y. Z. Li, W. J. Shi, L. Hou, Y. Y. Wang, Z. Zhu, Angew. Chem. Int. Ed. 2022, 61, e202213015; p) L. Gong, Y. Liu, J. Ren, A. M. Al-Enizi, A. Nafady, Y. Ye, Z. Bao, S. Ma, Nano Res. **2022**, *15*, 7559–7564.
- [12] a) Y. Zhang, J. Hu, R. Krishna, L. Wang, L. Yang, X. Cui, S. Duttwyler, H. Xing, Angew. Chem. 2020, 132, 17817–17822; b) Y. Zhang, L. Yang, L. Wang, S. Duttwyler, H. Xing, Angew. Chem. 2019, 131, 8229–8234; c) Y. Zhang, L. Yang, L. Wang, X. Cui, H. Xing, J. Mater. Chem. A 2019, 7, 27560–27566; d) Y. Zhang, L. Yang, L. Wang, S. Duttwyler, H. Xing, Angew. Chem. Int. Ed. 2019, 58, 8145–8150; e) Y. Zhang, J. Hu, R. Krishna,

- L. Wang, L. Yang, X. Cui, S. Duttwyler, H. Xing, *Angew. Chem. Int. Ed.* **2020**, *59*, 17664–17669; f) W. Sun, J. Hu, S. Duttwyler, L. Wang, R. Krishna, Y. Zhang, *Sep. Purif. Technol.* **2022**, *283*, 120220; g) W. Sun, Y. Jin, Y. Wu, W. Lou, Y. Yuan, S. Duttwyler, L. Wang, Y. Zhang, *Inorg. Chem. Front.* **2022**, *9*, 5140–5147.
- [13] a) H. C. Longuet-Higgins, M. d. V. Roberts, Proc. R. Soc. A-Math. Phys. Eng. Sci. 1955, 230, 110–119; b) J. Zhang, Z. Xie, Chem. Asian J. 2010, 5, 1742–1757.
- [14] a) Z. Qiu, Z. Xie, Acc. Chem. Res. 2021, 54, 4065–4079; b) H. Zhang, Z. Qiu, Z. Xie, Chin, J. Org. Chem. 2020, 40, 3203.
- [15] a) L. Wang, W. Sun, Y. Zhang, N. Xu, R. Krishna, J. Hu, Y. Jiang, Y. He, H. Xing, Angew. Chem. Int. Ed. 2021, 60, 22865–22870; b) R.-B. Lin, S. Xiang, H. Xing, W. Zhou, B. Chen, Coord. Chem. Rev. 2019, 378, 87–103.
- [16] M. Kirchmann, L. Wesemann, Dalton Trans. 2008, 2144–2148.
- [17] C. M. Breneman, K. B. Wiberg, J. Comput. Chem. 1990, 11, 361–373.
- [18] D. Tahaoğlu, F. Alkan, M. Durandurdu, J. Mol. Model. 2021, 27, 1-11.
- [19] a) R. S. Bakdash, I. Aljundi, C. Basheer, I. Abdulazeez, Sci. Rep. 2020, 10, 1–12; b) L. E. Gálvez-González, J. A. Alonso, L. O. Paz-Borbón, A. Posada-Amarillas, J. Phys. Chem. C. 2019, 123, 30768–30780.
- [20] M. J. Frisch, G. W. Trucks, H. B. Schlegel, G. E. Scuseria, M. A. Robb, J. R. Cheeseman, G. Scalmani, V. Barone, B. Mennucci, G. A. Petersson, H. Nakatsuji, M. Caricato, X. Li, H. P. Hratchian, A. F. Izmaylov, J. Bloino, G. Zheng, J. L. Sonnenberg, M. Hada, M. Ehara, K. Toyota, R. Fukuda, J. Hasegawa, M. Ishida, T. Nakajima, Y. Honda, O. Kitao, H. Nakai, T. Vreven, J. A. Montgomery, Jr., J. E. Peralta, F. Ogliaro, M. Bearpark, J. J. Heyd, E. Brothers, K. N. Kudin, V. N. Staroverov, R. Kobayashi, J. Normand, K. Raghavachari, A. Rendell, J. C. Burant, S. S. Iyengar, J. Tomasi, M. Cossi, N. Rega, J. M. Millam, M. Klene, J. E. Knox, J. B. Cross, V. Bakken, C. Adamo, J. Jaramillo, R. Gomperts, R. E. Stratmann, O. Yazyev, A. J. Austin, R. Cammi, C. Pomelli, J. W. Ochterski, R. L. Martin, K. Morokuma, V. G. Zakrzewski, G. A. Voth, P. Salvador, J. J. Dannenberg, S. Dapprich, A. D. Daniels, Ö. Farkas, J. B. Foresman, J. V. Ortiz, J. Cioslowski, D. J. Fox, GAUSSIAN09, Gaussian Inc., Wallingford, CT, USA, 2009.
- [21] a) S. Grimme, S. Ehrlich, L. Goerigk, J. Comput. Chem. 2011, 32, 1456–1465; b) C. Lee, W. Yang, R. G. Parr, Phys. Rev. B. 1988, 37, 785; c) J. Antony, S. Grimme, Phys. Chem. Chem. Phys. 2006, 8, 5287–5293; d) A. D. Becke, Phys. Rev. A. 1988, 38, 3098.
- [22] R. Dennington, T. Keith, J. Millam, GaussView. Semichem Inc. Shawnee Mission, KS. 2009.
- [23] K. Momma, F. Izumi, J. Appl. Crystallogr. 2011, 44, 1272-1276.
- [24] T. Lu, F. Chen, J. Comput. Chem. 2012, 33, 580-592.

Manuscript received: March 24, 2023 Revised manuscript received: May 24, 2023 Accepted manuscript online: May 30, 2023 Version of record online: July 17, 2023